Optical Materials 31 (2009) 1115–1117

Contents lists available at ScienceDirect

Optical Materials

journal homepage: www.elsevier.com/locate/optmat

Stable transparent Ni electrodes

Luis Martínez [a,*], Dhriti Sundar Ghosh [a], Stefano Giurgola [b], Paolo Vergani [b], Valerio Pruneri [a,c]

[a] ICFO-Institut de Ciencies Fotoniques, Mediterranean Technology Park, 08860 Castelldefels (Barcelona), Spain
[b] Avanex Corporation, Via Fellini 4, 20097 San Donato Milanese, Italy
[c] ICREA-Institució Catalana de Recerca i Estudis Avançats, 08010 Barcelona, Spain

ARTICLE INFO

Article history:
Received 22 October 2008
Received in revised form 26 November 2008
Accepted 27 November 2008
Available online 19 January 2009

ABSTRACT

We have deposited ultrathin (<10 nm) Ni films (UTMFs) on a dielectric substrate with high uniformity and investigated their stability, i.e. how their optical and electrical properties are affected by oxidation. We show that the oxidation process can be exploited to achieve stable films: an appropriate temperature cycle in the presence of oxygen produces a protective oxide layer on top of the metallic film which prevents further oxidation. The achieved stability, combined with large optical transmission and electrical conductivity, makes UTMFs high quality transparent electrodes for the optoelectronics industry, seriously competing with widely used transparent conductive oxides.

1. Introduction

Optically transparent and electrically conductive electrodes are of crucial importance for many photonic applications, such as solar cells, organic light emitting diodes (OLEDs), photodetectors, integrated modulators, electrochromic devices and flat panel displays. Up to now, major effort has concentrated to produce high quality transparent conductive oxides (TCOs), being indium tin oxide (ITO) the most widely used among them. Despite the excellent trade-off between electrical resistivity and optical transparency that can be achieved for ITO [1,2], drawbacks such as compatibility with organic materials [3], integration into industrial process flows and cost have led to the search of alternative materials, including zinc oxide [4], metal alloys [5], thin noble metal films [6], alkaline earth metals protected from oxidation by a thin noble metal layer [7], carbon nanotubes [8], multi-component metal films [9] and single-component ultrathin metal films (UTMFs) [10]. UTMFs based on transition metals overcome the high cost of raw materials such as indium (In) and noble metals and can be grown using a simple single process technique, i.e. sputtering, thus becoming a straightforward solution to be integrated into typical industrial process flows. In addition, contrary to TCOs, they possess high compatibility with nearly all organic and semiconductor materials (e.g. active medium) of the devices and related fabrication steps.

A potential drawback of UTMFs is the degradation they can undergo due to oxidation when exposed to environmental agents such as air, moisture and temperature. In fact, contact with other reactive chemical elements can also take place during fabrication (e.g. wet etching) or even be part of the structure of the device (e.g. metal/SiO_2). UTMFs are thus always at risk of changing their electrical and optical properties. In particular this is the case for not noble metallic layers, such as chromium (Cr), nickel (Ni), titanium (Ti) and aluminum (Al).

The purpose of this paper is twofold: on one hand we investigate the effect of oxidation on the electrical and optical properties of UTMFs while, on the other hand, we take advantage of it by inducing ad-hoc oxide protective layers, so that stable UTMFs can be produced. We focus our work on Ni films, which we subject to thermal treatment in either ambient atmosphere (~20% of O_2) or in the presence of a continuous O_2 flow. The obtained results and techniques can be extended to other metals, such as Cr, Ti and Al.

2. Experimental

Ultrathin Ni films were grown on a borosilicate glass (BK7) substrate using a *Kenosistec Dual Chamber DC sputtering system*. Deposition was performed in a pure argon (Ar) atmosphere at 8 mTorr pressure and 200 W of electric DC power were used. Several layers with different thicknesses, inferred from the deposition rate [10], were grown: 2.2, 3.4, 5.0 and 10.1 nm (from now on referred as samples A, B, C and D). Surface and optical transparency studies on as-deposited films were carried out using a contact mode *Digital Instrument Dimension 3100* Atomic Force Microscope (AFM) and a *Perkin–Elmer Lambda 950* spectrometer, respectively. In order to get continuous films, their RMS roughness has to be kept below the layer's thickness and consequently polished substrates with typical RMS roughness levels below 1 nm were employed. Fig. 1 shows a 3D AFM image of the surface of sample C obtained with the AFM associated software WSxM [11] with a corresponding RMS roughness of 0.3 nm and a peak-to-valley value of 1.7 nm.

Sheet resistance (R_S in Ω/□) measurements were performed using a *Cascade Microtech 44/7S 2791* four point probe connected

* Corresponding author.
E-mail address: luis.martinez@icfo.es (L. Martínez).

0925-3467/$ - see front matter © 2008 Elsevier B.V. All rights reserved.
doi:10.1016/j.optmat.2008.11.019

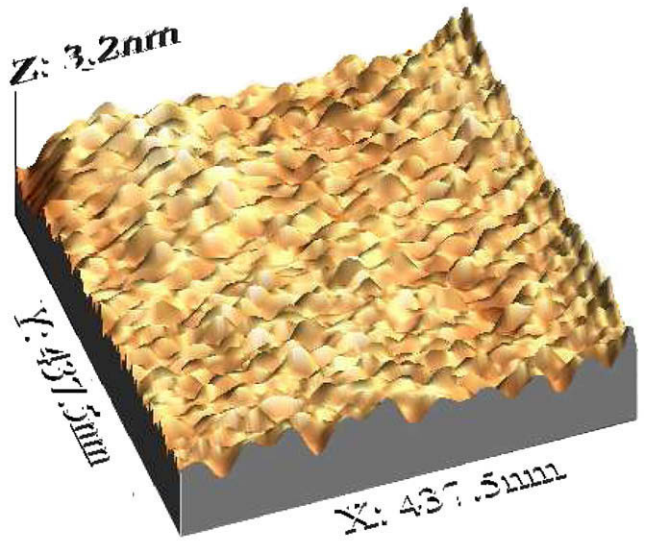

Fig. 1. Three-dimensional AFM image of sample C (Ni 5 nm). RMS roughness and a peak-to-valley level were found to be 0.3 and 1.7 nm, respectively, both being well below deposited thickness.

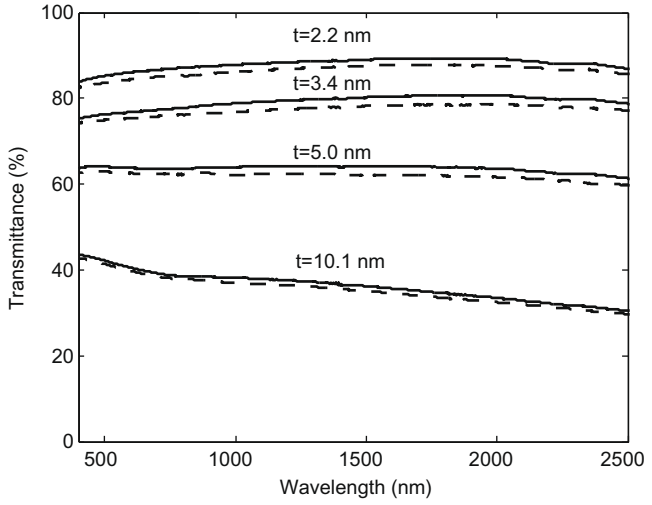

Fig. 3. Optical transparency in the 400–2500 nm of the films (dashed line was measured before the whole thermal treatment while solid line was obtained after H5 [after treatment]) on BK7 substrate. All the samples showed increased optical transmittance after treatment.

to a *Keithley 2001* multimeter. The film resistivity (ρ in Ω cm) can then be calculated as $\rho = R_S \times t$, where t is the thickness of the film. The as-deposited ρ values are 3,600,000 461, 153 and 53 $\mu\Omega$ cm for samples A, B, C and D, respectively. Sheet resistance measurements were repeated after keeping the films in ambient atmosphere for 12 days. The corresponding relative variation in electrical resistivity ($\Delta\rho/\rho$) in % for all the samples was the largest observed when compared to all subsequent treatments. In fact the sheet resistance of the thinnest sample A could not be measured any longer for its too high value, whereas samples B, C and D showed increases of 59%, 16% and 4%, respectively.

The subsequent thermal treatments with increasing temperature, H1 to H4 (inset of Fig. 2), were carried out in ambient atmosphere using a *Selecta Hightemp 2001406* oven. The temperature was measured using a *Fluke thermometer 52 II* connected to a *80 PK-1* thermocouple. The electrical resistivity kept increasing after each thermal treatment for samples B and C, this effect being larger for thinner films (Fig. 2) since the formation of a natural oxide layer due to oxygen indiffusion reduces the effective metallic path, thus leading to higher electrical resistivity (note that ρ is calculated from R_S using the initial thickness t). Indeed, changes for the thickest sample D were found to be negligible for all treatments. A final step (H5) identical to the first one (H1) was carried out at low temperature. As it can be observed in Fig. 2, contrary to the initial step (H1), the electrical resistivity changes due to H5 are negligible (within 2%) for all films, thus indicating that all UTMFs have reached high stability.

The optical transparency of all the samples was re-measured after the aforesaid thermal treatments using a *Perkin–Elmer Lambda 950* spectrometer and compared to that of as-deposited films (Fig. 3). All the samples showed increased transparency since metal oxides typically possess lower extinction coefficient than the original metals [12].

In order to further elucidate the mechanism and increase the speed of the oxidation leading to stability, we subjected new Ni films to thermal treatment under a controlled dry O_2 flux. Films

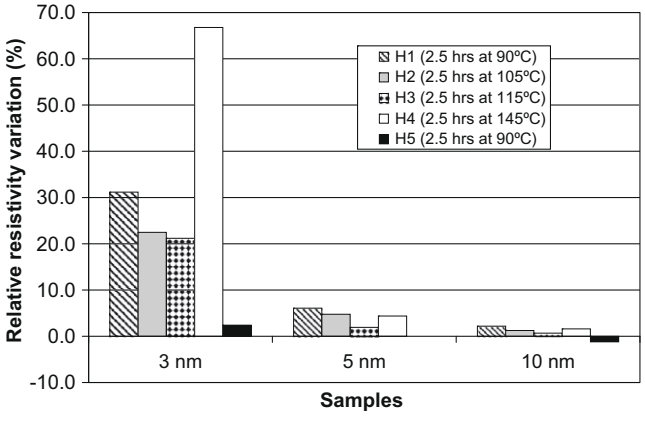

Fig. 2. Electrical resistivity variation after cumulative annealing treatments. After every step, the electrical resistivity of the samples increased, this effect being more significant for thinner films. After H5, all the samples showed negligible electrical resistivity changes, thus indicating that the films have reached stability. Note that the electrical resistivity variation on the 5 nm sample after H5 is very small and cannot be appreciated from the plot.

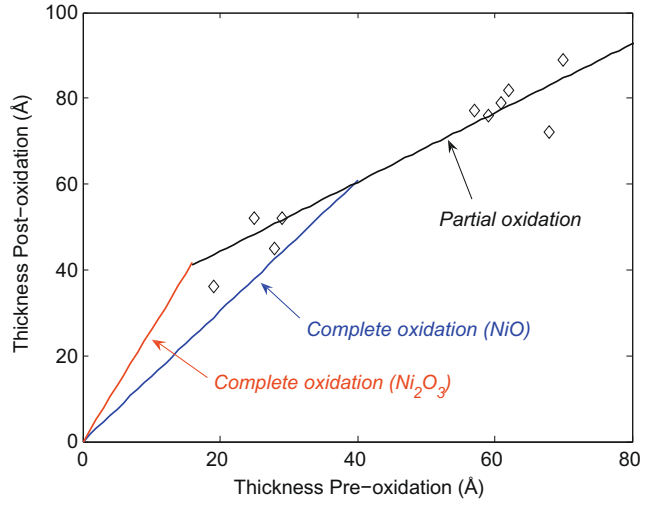

Fig. 4. Effect of oxidation on the thickness of nickel-based UTMFs. Since Ni has mainly two possible oxides (NiO and Ni_2O_3), both corresponding complete oxidation lines are given with slopes of 1.52 and 2.6, respectively.

Table 1
Molar mass and density of nickel and its main oxide compounds Ni(II) and Ni(III) [13]. Last column gives the ratio between the compound number of moles over that of Ni.

Element	Molar mass	Density	N_{ox}/N_{nickel}
Nickel	58.69	8.908	
NiO	74.71	7.45	1
Ni_2O_3	165.42	4.83	0.5

of different thickness were subjected to 90 min of degassing in vacuum at a temperature of about 140 °C and subsequently exposed to O_2 flux for 5 min by means of an ion gun (ion gun settings: 160 V acceleration potential and 1.8 A ion current).

The effect of oxidation can be estimated by evaluating the thickness variation of films, due to the formation of the corresponding metal oxide compound. Fig. 4 shows the thickness scatter plot of different samples before and after the whole oxidation treatment. In case of complete oxidation, and if the oxide compound is known, one can write the thickness ratio between metal and its oxide as:

$$\frac{t_{ox}}{t_m} = \frac{N_{ox}}{N_m}\frac{P_{ox}}{P_m}\frac{\delta_m}{\delta_{ox}} \quad (1)$$

where N is the number of moles, P is the molar mass and δ is the density of the material. Note that subscript m stands for metal and ox for the oxide. The main relevant parameters for Ni and its main oxide compounds are given in Table 1.

Given that Ni has two oxide compounds (NiO and Ni_2O_3), both corresponding complete oxidation lines are shown in Fig. 4 with slopes t_{ox}/t_m of 1.52 and 2.6, respectively. Completely oxidized films will increase their thickness according to a proportional factor within this interval, since the formation of a solid solution of both oxides might also be possible. However, in practice, oxidation is expected only up to a maximum thickness. Thicker layers should undergo partial oxidation for the same amount of metal thickness; in this case Eq. (1) will not hold. By fitting experimental data of thicker samples one obtains the partial oxidation line whose intersection point with the complete oxidation line represents the maximum oxidation thickness. According to thickness variations, the maximum oxidation thickness under the experimental conditions is in the range of 15–40 Å.

3. Conclusions

Oxides forming on UTMFs can be advantageously used to increase film stability. The resulting films present higher optical transparency while still preserving adequate electrical properties as long as the initial thickness is in the 3–10 nm range. These findings make UTMFs very attractive transparent electrodes for many applications. In fact, we have already demonstrated the use of the outlined approach to produce stable films for integrated modulators and OLEDs.

Acknowledgement

This work was partly supported by the Spanish National Program Plan Nacional No. TEC 2007-60185.

References

[1] C.G. Granqvist, Solar Energy Materials and Solar Cells 91 (2007) 1529.
[2] A. Amaral, P. Brogueira, C. Nunes de Carvalho, G. Lavareda, Optical Materials 17 (2001) 291.
[3] X. Jiang, F.L. Wong, M.K. Fung, S.T. Lee, Applied Physics Letters 83 (2003) 1875.
[4] H.K. Kim, K.S. Lee, J.H. Kwon, Applied Physics Letters 88 (2006) 012103.
[5] C.K. Wang, S.J. Chang, Y.K. Su, C.S. Chang, Y.Z. Chiou, C.H. Kuo, T.K. Lin, T.K. Ko, J.J. Tang, Material Science and Engineering B 112 (2004) 25.
[6] S. Conoci, S. Petralia, P. Samorì, F.M. Raymo, S. Di Bella, S. Sortino, Advanced Functional Materials 16 (2006) 1425.
[7] R.B. Pode, C.J. Lee, D.G. Moon, J.I. Han, Applied Physics Letters 84 (2004) 4614.
[8] Z. Wu, Z. Chen, X. Du, J.M. Logan, J. Sippel, M. Nikolou, K. Kamaras, J. Reynolds, D.B. Tanner, A.F. Hebard, A.G. Rinzler, Science 305 (2004) 1273.
[9] H.W. Jang, W. Urbanek, M.C. Yoo, J.L. Lee, Applied Physics Letters 80 (2002) 2937.
[10] S. Giurgola, A. Rodriguez, L. Martinez, P. Vergani, F. Lucchi, S. Benchabane, V. Pruneri, Journal of Materials Science: Materials in Electronics, Published online: 22 December 2007.
[11] I. Horcas, R. Fernández, J.M. Gómez-Rodríguez, J. Colchero, J. Gómez-Herrero, A.M. Baro, Review of Scientific Instruments 78 (2007) 013705.
[12] E.D. Palik, Handbook of Optical Constants of Solids, Academic Press, 1985.
[13] N.A. Lange, J.G. Speight, Lange's Handbook of Chemistry, 16th ed., McGraw-Hill, 2005.